MATERIALS PHYSICS AND MECHANICS RESEARCH ARTICLE

Submitted: July 31, 2025 **Revised: December 16, 2025** **Accepted: February 16, 2026**

Physical and mechanical properties of metallic cellular structures with "Gyroid" geometry

M.M. Sychov [1], P.A. Kuznetsov [2], S.V. Balabanov [3], V.V. Bobyr [2], T.V. Kniaziuk [2], A.S. Zhukov [2], A.M. Kuropiatnik [1] ✉, S.V. Diachenko [1]

[1] St. Petersburg Institute of Technology (Technical University), St. Petersburg, Russia

[2] NRC "Kurchatov Institute" – CRISM "Prometey", St. Petersburg, Russia

[3] Institute of Silicate Chemistry of the National Research Center "Kurchatov Institute", St. Petersburg, Russia

✉ artur.kuropiatnik@gmail.com

ABSTRACT

The use of selective laser melting for the manufacture of metal cells with the geometry of a triply periodic minimal surface 'gyroid' are discussed. The samples were made of 12Kh18N10T stainless steel. To study the effect of wall thickness on the physical and mechanical properties of materials with a triply periodic minimal surface geometry, a series of samples with dimensions of 30 × 30 × 30 mm^3, with wall thicknesses ranging from 0.1 to 0.8 mm and an elementary cell size of 10 × 10 × 10 mm^3. During the study, the specific energy absorption of the developed volumetric product obtained using additive technologies was evaluated. It was shown that the products have high strength and energy absorption characteristics necessary for use in many industries, and can also be used in protective structures.

KEYWORDS

additive technologies • cellular structures • gyroid geometry

Funding. *This work has been supported by the grant of the Russian Science Foundation, RSF 21-73-30019.*

Citation: Sychov MM, Kuznetsov PA, Balabanov SV, Bobyr VV, Kniaziuk TT, Zhukov AS, Kuropiatnik AM, Diachenko SV. Physical and mechanical properties of metallic cellular structures with "Gyroid" geometry. *Materials Physics and Mechanics.* 2026;54(4): 11–21.
http://dx.doi.org/10.18149/MPM.5442026_2

Introduction

Cellular materials find application in various industrial fields, such as aerospace engineering, thermal systems, packaging, and medical implants [1–6]. Such structures exhibit high energy-absorbing properties due to their high specific strength and ability to undergo large compressive strains [7–13].

Current trends in improving metallic protective structures are associated with the development of cellular materials featuring topologically optimized geometry [14]. One approach to optimizing lattice structures is the use of cellular materials with triply periodic minimal surface (TPMS) geometries, which enhance physical and mechanical properties [15–19]. Minimal surfaces are surfaces with zero mean curvature [20]; consequently, the load in such a system should be uniformly distributed, making TPMS-based materials promising for use under extreme loading conditions. Academician V.Ya. Shevchenko has demonstrated the effectiveness of TPMS-based materials under extreme loading conditions [21,22].

© M.M. Sychov, P.A. Kuznetsov, S.V. Balabanov, V.V. Bobyr, T.T. Kniaziuk, A.S. Zhukov, A.M. Kuropiatnik, S.V. Diachenko, 2026.
Publisher: Peter the Great St. Petersburg Polytechnic University
This is an open access article under the CC BY-NC 4.0 license (https://creativecommons.org/li-censes/by-nc/4.0/)

TPMSs were discovered and described by K.H.A. Schwarz in 1865 [23]. To control the mechanical behavior of cellular materials with TPMS geometry, the composition of the base material, the size and shape of the unit cell, and the wall thickness can be varied. It is known that such materials exhibit unique performance characteristics and are considered metamaterials, as their mechanical properties are largely determined by the geometry of the cellular structure [24]. However, the fabrication of components described by such complex curved surfaces remains a challenging task due to the technical limitations of conventional subtractive manufacturing methods [25]. The development of additive manufacturing technologies has made it possible to create and utilize components with TPMS geometry [26–28].

TPMS-based cellular materials can be used as a substrate in bilayer protective structures, the first layer of which may consist of ceramic materials. Ceramics possess high hardness [29,30] and, in such a composite, directly interact with penetrating objects such as bullets or fragments, effectively decelerating them, dissipating impact energy, distributing it over a larger area, and reducing localized effects. The ceramic layer absorbs a significant portion of the impact kinetic energy, often fracturing but preventing penetration or reducing the velocity of the projectile. Meanwhile, the metallic layer absorbs the remaining energy, as metals exhibit high ductility and can deform without fracturing [31]. Furthermore, the metallic layer provides structural support to the ceramic layer, which is more brittle and may crack or fracture upon impact.

TPMS are nature-inspired structures. For example, in living organisms, similar hierarchies are found in bone structure or in the wing structures of butterflies and dragonflies [32]. D. Mahmoud and M.A. Elbestawi have shown that TPMS can be used to develop artificial orthopedic implants with porosity comparable to that of human bone [33,34]. The porous structure facilitates bone ingrowth and strengthens the bond between the implant and the bone [35].

The aim of this work is to investigate the relationship between the wall thickness and the physical and mechanical properties of metallic energy-absorbing materials with "Gyroid" TPMS geometry.

Materials and Methods

Development of 3D Models

For the "Gyroid" geometry, the surface equation can be defined analytically using the following expression:

$$\cos(x) \cdot \sin(y) + \cos(y) \cdot \sin(z) + \cos(z) \cdot \sin(x) = 0. \quad (1)$$

To investigate the influence of the TPMS structure type and wall thickness on the properties of components with TPMS geometry, a series of 3D models of specimens was developed. The curved surfaces that define the 3D models with "Gyroid" geometry [36,37] were generated using parametric modeling in RhinoCeros 3D software (Figs. 1 and 2) in accordance with Eq. (1). The "offsetmesh" command was used to impart the required wall thickness to the specimens. RhinoCeros 3D is a software program for 3D graphics and computer-aided design (CAD), widely used in architecture, jewelry design, and industrial design. To investigate the influence of wall thickness on the physical and mechanical properties of materials with TPMS geometry, a series of specimens with "Gyroid"

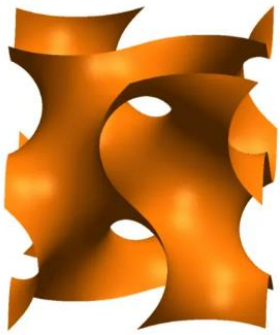


Fig. 1. Gyroid unit cell

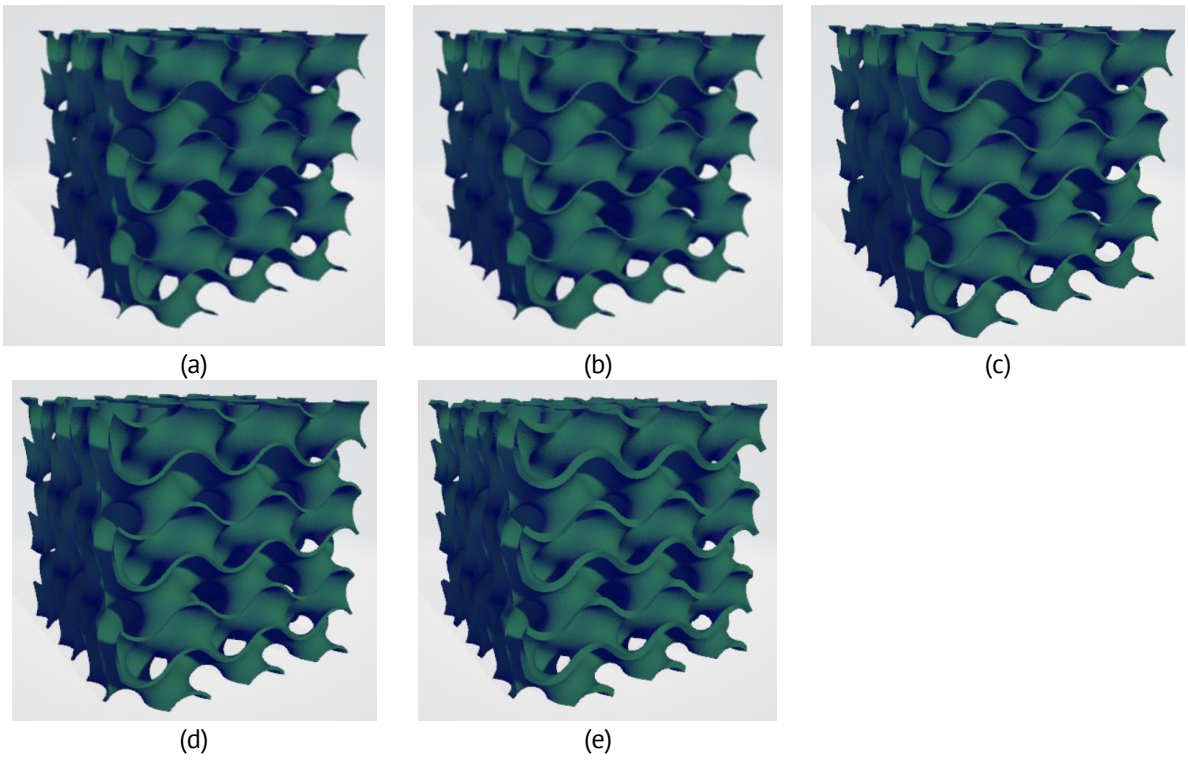


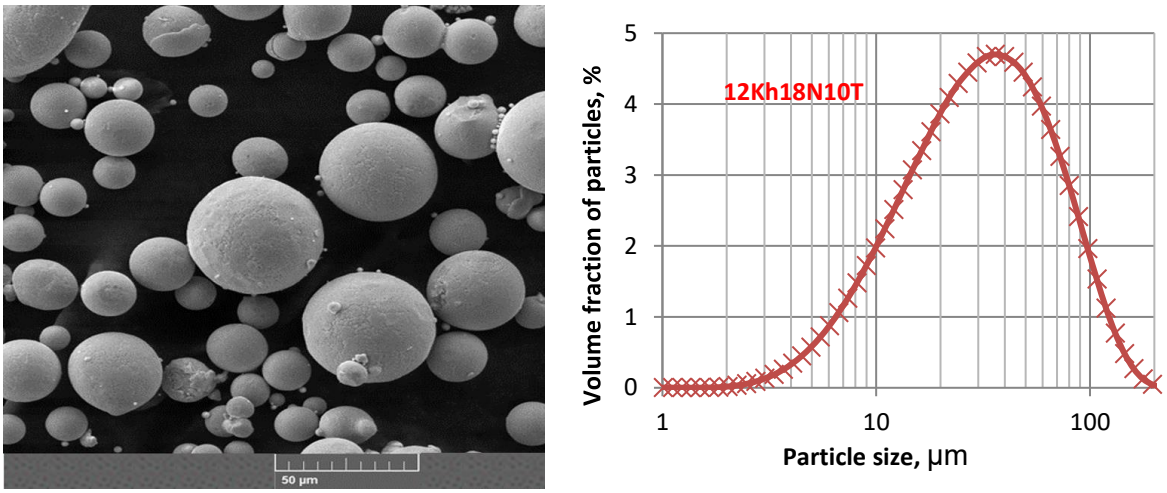
Fig. 2. 3D models of specimens with different wall thicknesses:
(a) 0.1 mm; (b) 0.2 mm; (c) 0.3 mm; (d) 0.4 mm; (e) 0.8 mm

geometry was manufactured with dimensions of 30 × 30 × 30 mm^3, wall thicknesses ranging from 0.1 to 0.8 mm, and a unit cell size of 10 × 10 × 10 mm^3.

3D printing of specimens

The fabrication of products with complex geometric shapes based on designed digital models is of high practical and scientific interest. One of the promising methods for their fabrication is the additive technique of selective laser melting (SLM) of powders [38,39]. This method involves the layer-by-layer synthesis of metallic components. Laser radiation selectively melts a layer of metal powder according to the specified model, ensuring the formation of parts with a microstructure distinct from that produced by conventional metalworking technologies. The application of this technique enables the production of structures with complex configurations and optimized mechanical characteristics, which is finding widespread application in various industries.

Powder of 12Kh18N10T stainless steel manufactured by Polema JSC, Tula (TU 14-22-266-2016), was used as the raw material for specimen fabrication. A micrograph and the particle size distribution curve of the powder are presented in Fig. 3. Table 1 presents the properties of the steel powder used.



(a) (b)

Fig. 3. Metal powder of 12Kh18N10T steel: (a) SEM image of particles; (b) differential particle size distribution curve

Table 1. Properties of 12Kh18N10T steel powder

Parameter	Quantile, μm			Flowability (50 g), s	ρ_b, g/cm³
	D_{10}	D_{50}	D_{90}		
Value	9.70	30.90	80.40	19.39	4.78

Table 2. Tensile test results according to GOST 1497-2023

Specimen No.	Build direction	Ultimate tensile strength, MPa	Yield strength, MPa	Elongation, %	Area reduction, %
1	Horizontal (perpendicular to the loading axis)	530	330	27	50
2		540	340	36	67
3		550	350	33	63
Average		540	340	32	60
4	Vertical (along the loading axis)	530	340	46	70
5		520	340	44	49
6		460	300	51	58
Average		503	327	47	59

Table 3. Impact bending test results according to GOST 9454-78

Specimen No.	Build direction	Impact energy, J	Impact strength, J/cm²
1	Vertical (along the loading axis)	146.6	182
2		132.7	164
3		126.3	157
4		122.8	155
5		127.4	158
6		140.5	176
Average		132.7	165

The powder particles are predominantly spherical with a regular shape; however, a small number of defective granules are present. On the surface of these defective granules, satellites (small particles that adhere to larger ones as a result of collisions during powder manufacturing) are present, along with granules having a non-spherical shape. The physical and mechanical properties of specimens fabricated from 12Kh18N10T steel without additional heat treatment are presented in Tables 2 and 3.

The specimens were fabricated using an EOSINT M270 system by the SLM method in accordance with the developed digital models (Fig. 2). Powder melting was carried out in a nitrogen atmosphere using a laser power of 195 W and a scanning speed of 800 mm/s; the thickness of the melted layer was 40 μm [40,41]. To investigate the physical and mechanical properties of metallic specimens with "Gyroid" geometry, specimens with wall thicknesses of 0.1, 0.2, 0.3, 0.4, and 0.8 mm were printed using the described technology. To determine the mechanical properties of the Gyroid structures, quasi-static compression testing was performed. The tests were conducted using a Zwick Z400E universal testing machine in accordance with GOST 25.503-97[1], at a constant loading rate of 5 mm/min (approximately 20.8 % strain per minute) at room temperature. The load was applied along the build direction of the specimens, since specimens produced by additive manufacturing exhibit their highest strength in this direction.

Results and Discussion

As a result of 3D printing, TPMS specimens with high fidelity to the intended geometry were fabricated. A noticeable deviation of the actual mass from the calculated value, up to 30 %, is observed only for specimens with the minimum wall thickness (0.1 mm), which is attributed to the fact that the wall thickness corresponds to approximately 2...3 particle diameters of the powder used. For the remaining specimens, the actual and calculated masses differ insignificantly (less than 3.5 %) (Fig. 4), which confirms the high accuracy of

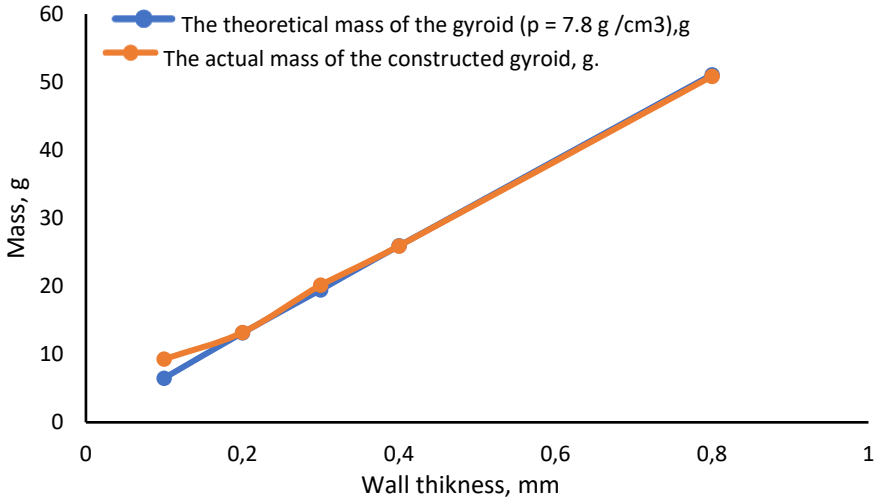


Fig. 4. Calculated and actual mass of specimens fabricated with different wall thicknesses: 0.1, 0.2, 0.3, 0.4, and 0.8 mm

[1] Interstate Standard. GOST 25.503-97. *Design calculation and strength testing. Methods of mechanical testing of metals. Method of compression testing.* Minsk, Belarus Republic: Interstate Council for Standardization, Metrology, and Certification; 1999.

the SLM method. This indicates that the printing process is capable of reproducing complex geometric structures with minimal deviations from the pre-designed parameters, which is critically important for applications requiring strict dimensional and mass conformity.

The stress-strain curves of the specimens are presented in Fig. 5. All curves can be divided into three characteristic regions: (1) a linear region (elastic strain zone), (2) a long wavy region (elastoplastic strain zone), (3) an exponentially increasing curve (plastic deformation zone – densification).

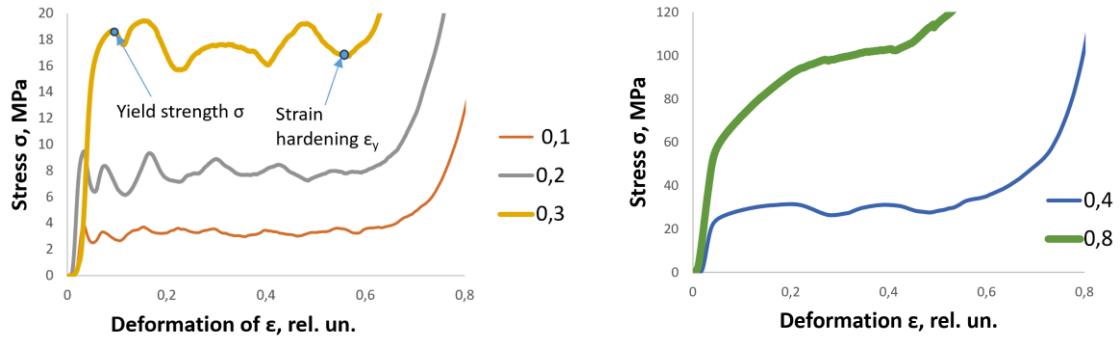


Fig. 5. Compressive stress-strain curves of specimens with "Gyroid" geometry and different wall thicknesses: (a) 0.1, 0.2, 0.3 mm; (b) 0.4, 0.8 mm

The linear-elastic region is observed up to 3–5 % strain; then the cells of the "Gyroid" geometry specimen undergo plastic deformation, resulting in a characteristic wavy region on the strain curve. The shape of the plateau region characterizes the progressive collapse of the unit cells and depends on the type of structural material and the cell geometry. After reaching the densification point (ε_d), a sharp increase in stress is observed, caused by the transition from deformation of the structure to deformation of the monolithic material. Thus, the densification point characterizes the limiting state of suitability of the structure as an energy-absorbing element.

Analysis of the stress-strain curves (Fig. 5) shows that they exhibit repeated stress maxima, the number of which depends on the wall thickness of the specimen. Thus, specimens with a wall thickness of 0.1 and 0.2 mm exhibit five maxima, those with a wall thickness of 0.3 mm exhibit four, those with 0.4 mm exhibit three, and the specimen with a wall thickness of 0.8 mm exhibits a single maximum, making its deformation behavior comparable to that of a monolithic specimen. Increasing the wall thickness of the unit cell leads to an enhancement of the strength properties of the specimen. Consequently, under compression, specimens with Gyroid geometry are characterized by layer-by-layer deformation, which is attributable to the features of the TPMS cellular structure. This structure ensures a uniform distribution of mechanical stresses throughout the volume of the material, resulting in sequential bending and collapse upon application of a compressive load. Such behavior is reflected in the formation of multiple maxima on the stress-strain curves, demonstrating the high energy absorption capacity of the material and its effectiveness under dynamic loading conditions. Crushing of the metamaterial begins when the ultimate strength σ is reached and ends upon final “collapse” and densification of the specimen (ε_d) (Fig. 5).

It is known that materials with TPMS geometry possess a high capacity for dissipating various forms of energy, including mechanical energy [42,43]. In [43], it is shown that such materials can be used to create passive safety components in various modes of transport. To evaluate the energy-absorbing capacity of cellular materials, the value of "energy absorption at 30 % strain" A_{30}, normalized to the mass of the tested specimen, is often used. The strain degree of the specimen is calculated using the following equation:

$$\varepsilon = \frac{\varepsilon_1}{\varepsilon_0} \cdot 100\%. \quad (2)$$

The specific energy absorption (normalized by mass) is calculated using the equation [43]:

$$A_m = \frac{1}{M} \int_{\varepsilon_0}^{\varepsilon_1} N \; d\varepsilon, \quad (3)$$

where N is the load, ε is the strain, M is the mass of the specimen.

From Eq. (3), it follows that the amount of energy absorption is the area under the stress-strain curve; therefore, for efficient operation of energy absorbers, both high strength and the ability to undergo large deformations are required. From the analysis of the stress-strain curves, the effective elastic and strength characteristics of the metamaterials under consideration were obtained (Table 4).

Table 4. Effective elastic and strength characteristics of the tested specimens

Wall thickness, mm	Ultimate strength σ, MPa	Young's modulus E, MPa	Energy absorption at 30 % strain A_{30}, MJ/m³
0.1	3.25	211.5	0.97
0.2	7.80	541.2	2.27
0.3	16.85	865.4	4.84
0.4	28.20	1250.7	8.04
0.8	95.00	1999.3	22.95

From the image of the macroetched section of the tested specimen (Fig. 6), it follows that during testing the specimen deformed layer-by-layer, and the structure of the specimens exhibits virtually no internal defects. This explains the formation of multiple peaks on the stress-strain curve.

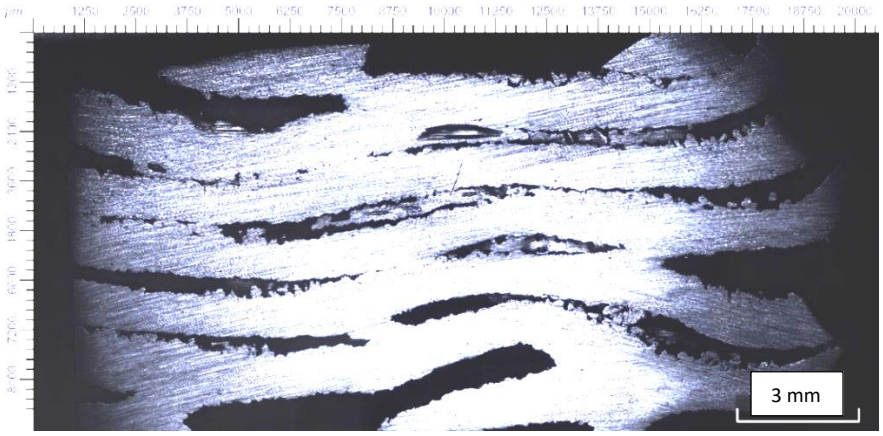


Fig. 6. Macroetched section of the specimen after compression (wall thickness 0.8 mm)

As the wall thickness increases, the energy-absorbing capacity (the amount of energy absorption normalized by mass) of the cellular structure with TPMS geometry increases according to a power-law relationship (Fig. 7). When the energy absorption of

the material is normalized by volume, the exponent changes (> 1), reflecting the nature of the increase in energy absorption (Fig. 8). According to Fig. 8, the dependence of

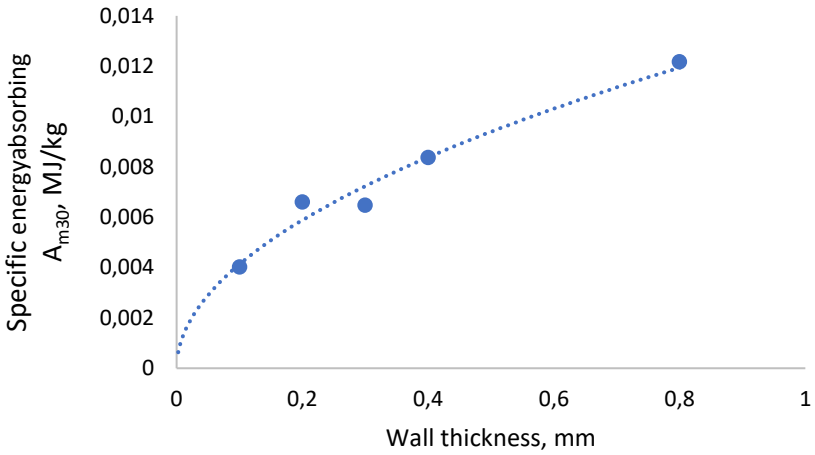


Fig. 7. Specific energy absorption of specimens at 30 % strain as a function of the wall thickness

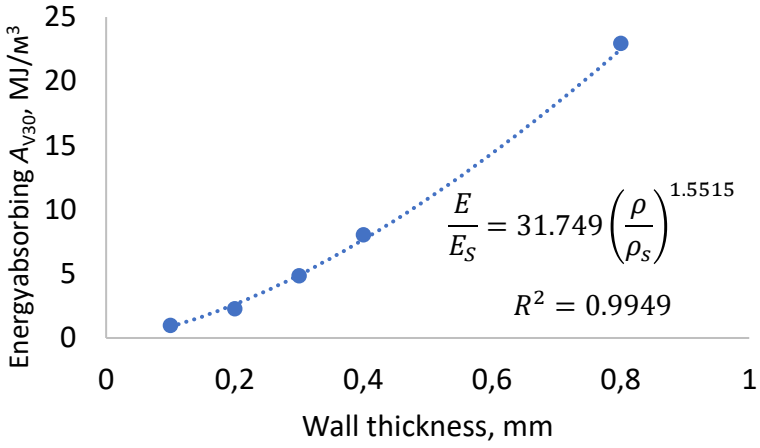


Fig. 8. Volumetric specific energy absorption of the material with "Gyroid" geometry at 30 % strain as a function of wall thickness

the volumetric specific energy absorption A_{V30} on the wall thickness of the cellular material follows a power law, as do many other physical and mechanical characteristics that can be described by the Gibson-Ashby equation [44]. The Gibson–Ashby equation is used to describe the mechanical properties of porous materials, such as foams or cellular structures. It relates the mechanical properties of a material (e.g., Young's modulus or strength) to its relative density (the fraction of solid material within the structure). The Gibson–Ashby equation is widely used in materials science for the design and analysis of porous materials.

The basic form of the Gibson–Ashby equation for the Young's modulus E is as follows:

$$\frac{E}{E_S} = \mathrm{C}\left(\frac{\rho}{\rho_s}\right)^n, \quad (4)$$

where E is the Young's modulus of the porous material (apparent modulus), E_s is the Young's modulus of the solid matrix material (solid phase), ρ is the density of the porous material, ρ_s is the density of the matrix material.

Based on Eq. (4), it can be concluded that the relationships presented in Figs. 7 and 8 express the Gibson–Ashby equations for cellular materials with "Gyroid" geometry. According to the test results, the energy absorption at 30 % strain of the studied metallic specimens with "Gyroid" geometry reaches 23 MJ/m³ (0.012 MJ/kg) at a wall thickness of 0.8 mm, which is higher than the known values for classical cellular structures in the form of honeycombs — 15...18 MJ/m³ [45].

Conclusions

As a result of 3D printing, TPMS specimens with high fidelity to the intended geometry were obtained. A noticeable deviation of the actual mass from the calculated value is observed only for specimens with the minimum wall thickness (0.1 mm). For the remaining specimens, the actual and calculated masses are virtually identical, which confirms the high accuracy of the SLM method as well as the comparable density of the material. Consequently, the printing process is capable of reproducing complex geometric structures with minimal deviations from the pre-designed parameters, which is critically important for applications requiring strict dimensional and mass conformity. Within the framework of this study, SLM technology was successfully implemented as a tool for manufacturing 3D metallic periodic structures possessing low weight and high strength and energy-absorbing characteristics.

It has been shown that SLM is an effective method for creating cellular materials with "Gyroid" TPMS geometry from 12Kh18N10T steel powder. The materials exhibit high energy absorption capacity due to the alternating processes of bending deformation, crushing, and compression. It was determined that the wall thickness of specimens with "Gyroid" geometry affects their strength, specifically, the greater the wall thickness, the higher the strength and the greater the energy absorption. Thus, by varying the wall thickness of the metamaterial, the desired specific parameters can be achieved. It has been shown that, along with the strength and the Young's modulus, the specific energy absorption of the cellular material also follows the Gibson–Ashby equation.

Given that the specific energy absorption of the developed material is significantly higher than the known values for classical cellular structures with hexagonal cells, it can be concluded that the developed materials can be used in ballistic protective systems due to their high energy-absorbing properties and ability for layer-by-layer deformation. These characteristics enable Gyroid structures to effectively dissipate impact energy, making them suitable for use in lightweight armored structures where a combination of low weight and high strength is essential. However, for implementation in ballistic protection, such cellular structures must be further optimized with respect to wall thickness and the materials used to ensure adequate protection against penetrating impacts.

CRediT authorship contribution statement

Maxim M. Sychov: writing – review & editing, writing – original draft; **Pavel A. Kuznetsov**: writing – original draft; **Sergey V. Balabanov**: writing – review & editing; **Vitaliy V. Bobyr**: writing – original draft; **Tatiana V. Kniaziuk**: writing – original draft; **Anton S. Zhukov**: writing – original draft; **Artur M. Kuropiatnik**: writing – original draft; **Semen V. Diachenko**: writing – review & editing.

Conflict of interest

The authors declare that they have no conflict of interest.

References

1. Plessis A, Razavi N, Benedetti M, Murchio S, Leary M, Watson M, Bhate D, Berto F. Properties and applications of additively manufactured metallic cellular materials: A review. *Progress in Materials Science*. 2022;125: 100918.
2. Murr LE, Gaytan SM, Medina F, Lopez H, Martinez E, Machado BI, Hernandez DH, Martinez L, Lopez MI, Wicker RB, Bracke J. Next-generation biomedical implants using additive manufacturing of complex, cellular and functional mesh arrays. *Philosophical Transactions of the Royal Society A: Mathematical, Physical and Engineering Sciences*. 2010;368(1917): 1999–2032.
3. Velu R, Calais T, Jayakumar A, Raspall FA. Comprehensive Review on Bio-Nanomaterials for Medical Implants and Feasibility Studies on Fabrication of Such Implants by Additive Manufacturing Technique. *Materials*. 2020;13(1): 92.
4. Sysoev EI, Sychov MM, Shafigullin LN, Dyachenko SV. Design of sound absorbing honeycomb materials with a geometry of triply periodic minimal surfaces (TPMS). *Acoustical Physics*. 2024;70: 887–898.
5. Bobyr V, Zhukov A, Shakirov I, Kuznetcov P. Selection of the selective laser melting modes – as the method of achieving an item's complex shape with the specified physical and mechanical properties. *Materials Today: Proceedings*. 2019;19(5): 2129–2133.
6. Yeranee K, Rao YA. Review of Recent Investigations on Flow and Heat Transfer Enhancement in Cooling Channels Embedded with Triply Periodic Minimal Surfaces (TPMS). *Energies*. 2022;15(23): 8994.
7. Shi X, Liao W, Li P, Zhang C, Liu T, Wang C, Wu J. Comparison of Compression Performance and Energy Absorption of Lattice Structures Fabricated by Selective Laser Melting. *Advanced Engineering Materials*. 2020;22(11): 2000453.
8. Ashokkumar CN, Vijayasimha Reddy BG, Chandrasekhar U. Impact energy absorption characteristics of 3-D printed AlSi10Mg TPMS gyroid metallic structures. *European Chemical Bulletin*. 2023;12(5): 1446–1452.
9. Kuznetcov P, Deev A, Staritcyn M, Zhukov A, Bobyr V. Energy absorbing properties of the cellular structures with different wall thickness, produced by the selective laser melting. *Materials Science Forum*. 2018;933: 330–336.
10. Yao B, Ye R, Li Z, Liu M, Liu Y. Compressive properties and energy absorption of honeycomb filled square tubes produced by selective laser melting. *Materials Science and Engineering: A*. 2022;847: 143259.
11. Arsentev MY, Sysoev EI, Vorobyov SA, Balabanov SV, Diachenko SV, Sychov MM, Skorb EV. Crystal-inspired cellular metamaterials with reduced Poisson's ratio as analogues of TPMS. *Composite Structures*. 2025;363: 119097.
12. Zhao M, Liu F, Fu G, Zhang DZ, Zhang T, Zhou H. Improved Mechanical Properties and Energy Absorption of BCC Lattice Structures with Triply Periodic Minimal Surfaces Fabricated by SLM. *Materials*. 2018;11(12): 2411.
13. Zobacheva AU, Nemov AS, Borovkov AI, Novokshenov AD, Khovaiko MV, Ermolenko NA. Design and simulation of additive manufactured structures of three-component composite material. *Materials Physics and Mechanics*. 2017;34(1): 51–58.
14. Montemurro M, Bertolino G, Panettieri E. Topology optimisation of architected cellular materials from additive manufacturing: Analysis, design, and experiments. *Structures*. 2023;47: 2220–2239.
15. Feng J, Fu J, Yao X, He Y. Triply periodic minimal surface (TPMS) porous structures: from multi-scale design, precise additive manufacturing to multidisciplinary applications. *International Journal of Extreme Manufacturing*. 2022;4(2): 022001.
16. Gado MG, Al-Ketan O, Aziz M, Al-Rub R, Ookawara S. Triply Periodic Minimal Surface Structures: Design, Fabrication, 3D Printing Techniques, State-of-the-Art Studies, and Prospective Thermal Applications for Efficient Energy Utilization. *Energy Technology*. 2024;12(5): 2301287.
17. Cheng Q, Yin J, Wen J, Yu D. Triply periodic minimal surface structures: Energy absorption performance under impact loading and their graded design. *Mechanics of Advanced Materials and Structures*. 2023;31(29): 11725–11736.
18. Diachenko SV, Dolgin AS, Khristyuk NA, Lebedev LA, Nefedova LA, Pavlov SB, Merenkov KF, Ivkov VI, Dmitrieva AN. 3D Printing of Ceramic Elements with Q-Surface Geometry for the Fabrication of Protective Barrier. *Ceramics*. 2023;6(2): 912–921.
19. Qureshi ZA, Al-Omari SAB, Elnajjar E, Al-Ketan O, Al-Rub RA. Nature-inspired triply periodic minimal surface-based structures in sheet and solid configurations for performance enhancement of a low-thermal-conductivity phase-change material for latent-heat thermal-energy-storage applications. *International Journal of Thermal Sciences*. 2022;173: 107361.
20. Dierkes U, Hildebrandt S, Sauvigny F. *Minimal Surfaces*. Heidelberg: Springer; 2010.

21. Shevchenko VYa, Sychev MM, Lapshin AE, Lebedev LA. Keramicheskiye materialy s topologiyey trizhdy periodicheskikh poverkhnostey minimalnoy energii dlya konstruktsiy, rabotayushchikh v usloviyakh ekstremalnykh nagruzheniy. *Fizika i khimiya stekla.* 2017;43(6): 640–643. (In Russian)
22. Shevchenko VYa, Sychev MM, Makogon AI. Modelirovaniye reaktsionno-diffuzionnykh protsessov formirovaniya kompozitov almaz–karbid kremniya. *Fizika i khimiya stekla.* 2021;47(4): 376–387. (In Russian)
23. Neovius ER. *Bestimmung zweier spezieller periodischer Minimal Flächen*. Helsingfors: Akad. Abhandlungen; 1883.
24. Borovkov AI, Maslov LB, Zhmaylo MA, Tarasenko FD, Nezhinskaya LS. Finite element analysis of elastic properties of metamaterials based on triply periodic minimal surfaces. *Materials Physics and Mechanics*. 2024;52(2): 11–29.
25. Balabanov S, Sychov M, Koshevaya K, Makogon A, Gravit M. Study of isotropy of mechanical properties of the TPMS-based cellular structures. *E3S Web of Conferences*. 2022;363: 04053.
26. Sychev MM, Lebedev LA, Dyachenko SV, Nefedova LA, Baygildin VA. *Additivnyye tekhnologii*. Sankt-Peterburg: SPbGTI(TU); 2018. (In Russian)
27. Afshar M, Pourkamali-Anaraki A, Montazerian H, Kadkhodapour J. Additive manufacturing and mechanical characterization of graded porosity scaffolds designed based on triply periodic minimal surface architectures. *Journal of the Mechanical Behavior of Biomedical Materials*. 2016;62: 481–494.
28. Maevskaia E, Guerrero J, Ghayor C, Bhattacharya I, Weber FE. Triply Periodic Minimal Surface-Based Scaffolds for Bone Tissue Engineering: A Mechanical, In Vitro and In Vivo Study. *Tissue Engineering Part A*. 2023;29(19–20): 507–517.
29. Matsui K, Hosoi K, Feng B, Yoshida H, Ikuhara Y. Ultrahigh toughness zirconia ceramics. *Proceedings of the National Academy of Sciences*. 2023;120(27): e2304498120.
30. Zaitsev A, Arutyunyan N, Koldaev A. Hot Ductility, Homogeneity of the Composition, Structure, and Properties of High-Strength Microalloyed Steels: A Critical Review. *Metals*. 2023;13(6): 1066.
31. Holdsworth S. Creep-Ductility of High Temperature Steels: A Review. *Metals*. 2019;9(3): 342.
32. Schroeder TBH, Houghtaling J, Wilts BD, Mayer M. It's Not a Bug, It's a Feature: Functional Materials in Insects. *Advanced Materials*. 2018;30(19): 1705322.
33. Mahmoud D, Elbestawi MA. Lattice Structures and Functionally Graded Materials Applications in Additive Manufacturing of Orthopedic Implants: A Review. *Journal of Manufacturing and Materials Processing*. 2017;1(2): 13.
34. Kilina P, Kuchumov AG, Sirotenko L, Vassilouk V, Golovin S, Drozdov A, Sadyrin EV. Influence of porous titanium-based jaw implant structure on osseointegration mechanisms. *Journal of the Mechanical Behavior of Biomedical Materials*. 2024;160: 106724.
35. Holmes DW, Singh D, Lamont R, Daley R, Forrestal DP, Slattery P, Pickering E, Paxton NC, Powell SK, Woodruff MA. Mechanical behaviour of flexible 3D printed gyroid structures as a tuneable replacement for soft padding foam. *Additive Manufacturing*. 2022;50: 102555.
36. Diachenko SV, Lebedev LA, Sychev MM, Nefedova LA. Physicomechanical Properties of a Model Material in the Form of a Cube with the Topology of Triply Periodic Minimal Surfaces of the Gyroid Type. *Technical Physics*. 2018;63: 984–987.
37. Deckard CR, Clemson SC. *Apparatus for producing parts by selective sintering.* US5597589A, 28 January 1997.
38. Meiners W, Wissenbach K, Gasser A. Shaped body especially prototype or replacement part production. DE19649865C1, 12 February 1996.
39. Dyachenko SV, Khristyuk NA, Bogdanova YeK, Gallyamova DR, Dmitrieva AN, Pavlov SB, Nefedova LA. K voprosu primeneniya nerzhaveyushchey stali 12Kh18N10T v selektivnom lazernom splavlenii. In: Chaika TV. (Eds.) *Perspektivnyye tekhnologii i materialy: Materialy Mezhdunarodnoy nauchno-prakticheskoy konferentsii. 21–23 Sentybrya 2022, Sevastopol*. Sevastopol: Sevastopolskii Gosudarstenni Universitet; 2022. p.195–198. (In Russian)
40. Zhukov AS, Shakirov IV, Kuznetcov PA, Sychev MM, Dyachenko SV, Nefedova LA. Comparison of the properties of additive materials obtained from sprayed powders of steels of various metallurgical production methods. *AIP Conference Proceedings*. 2021;2402(1): 60021.
41. Zhao J, Li M, Chen J, Gao W, Bai H. Energy-absorbing porous materials: Bioinspired architecture and fabrication. *Nano Research*. 2024;17: 679–690.
42. Shevchenko V, Balabanov S, Sychov M, Karimova L. Prediction of Cellular Structure Mechanical Properties with the Geometry of Triply Periodic Minimal Surfaces (TPMS). *ACS Omega*. 2023;8(30): 26895–26905.
43. Balabanov SV, Makogon AI, Sychev MM, Evstratov A, Regazzi A, Lopez-Cuesta JM. 3D Printing and Mechanical Properties of Polyamide Products with Schwartz Primitive Topology. *Technical Physics*. 2020;65: 211–215.
44. Gibson LJ, Ashby MF. The Mechanics of Three-Dimensional Cellular Materials. *Proceedings of the Royal Society of London*. 1982;382(1782): 43–59.
45. Markov VA, Pusev VI, Selivanov VV. Voprosy primeneniya vysokoporistykh metallov i sotovykh konstruktsiy dlya zashchity ot udarnovolnovykh nagruzok. *Voprosy Oboronnoy Rekhniki*. 2012;7–8: 54–62. (In Russian)